

# High-Resolution Solid-State NMR Study of the Occurrence and Thermal Transformations of Silicon-Containing Species in Biomass Materials

Jair C. C. Freitas,<sup>\*,†,‡</sup> Francisco G. Emmerich,<sup>†</sup> and Tito J. Bonagamba<sup>§</sup>

*Departamento de Física, Universidade Federal do Espírito Santo, 29060–900 Vitória, ES, Brazil; Departamento de Matéria Condensada e Espectroscopia, Centro Brasileiro de Pesquisas Físicas, 22290-180 Rio de Janeiro, RJ, Brazil; and Instituto de Física de São Carlos, Universidade de São Paulo, P.O. Box 369, 13560–970 São Carlos, SP, Brazil*

*Received July 26, 1999. Revised Manuscript Received October 21, 1999*

The occurrence of silicon in two kinds of biomass (rice hulls and endocarp of babassu coconut) and the thermal transformations taking place in these materials under heat treatments are studied here. We report also the production, characterization, and study of carbonaceous materials with high SiC content through the carbothermal reduction of silica, using these natural precursors. X-ray diffraction, scanning electron microscopy, and <sup>13</sup>C and <sup>29</sup>Si room temperature high-resolution solid-state NMR measurements are used in the characterization and study of the materials as well as the process of SiC formation. Important conclusions about the nature of silicon in these types of biomass and the effects of heat treatments on the structure of silicon-containing species are derived from the results presented. It is shown that silicon in these materials occurs in two distinct forms: amorphous hydrated silica and organically bound silicon species. The influence of spin–lattice relaxation dynamics on the NMR spectra is discussed, evidencing the role played by the paramagnetic defects produced in the materials through pyrolysis.

## Introduction

A great deal of interest in the occurrence of silicon in rice hulls (RH) has arisen in the past several years due to the possibility of the synthesis of silicon carbide (SiC), silicon nitride (Si<sub>3</sub>N<sub>4</sub>), high-purity silica, and other materials through their thermal decomposition. The use of an inexpensive waste product of the agricultural industry such as rice hulls in the process of synthesis of these important technological products has been attractive both from the economical and the ecological point of view. The formation of SiC from rice hulls was first reported by Lee and Cutler<sup>1</sup> and since then, a large number of works has been published about this topic.<sup>2–7</sup> The most commonly used process is the heat treatment of rice hulls at temperatures above 1200 °C under vacuum or argon atmosphere, where the formation of SiC takes place from the reaction between silica and carbon present in the material. The intimacy of the contact between silica and carbon, as well as the amor-

phous and reactive nature of these species in rice hulls, allows this reaction to occur at temperatures below those used for the reaction between crystalline silica and graphite.<sup>1,3,7</sup>

Since the early 1960s, the occurrence of silicon in rice and other plants has been investigated by chemists and biologists.<sup>8–11</sup> Attempts have been made in order to understand the nature and distribution of the silicon species through the rice plant, noticeably in the rice hulls. The prevailing conclusion was that silicon occurred in rice hulls in a hydrated amorphous form, either opal or silica gel, located mainly in the outer epidermis and filling up the intraspaces in the spiral structure of the epidermal cells.<sup>8,10</sup> Liu and Ho proposed, on the basis of solubility studies, that part of the silica might be organically combined with carbohydrates and concluded that “silicon in rice hull is different from silica”.<sup>9</sup>

The investigation of the nature and location of silicon in rice hulls was revisited by Sharma et al.<sup>12</sup> in connection with a study about the production of SiC whiskers. They found that silicon occurs in rice hulls mainly in the form of SiO<sub>2</sub> tetrahedra and from Auger electron spectroscopy results concluded that silica was presumably bound to carbohydrates, reinforcing the conclusions of Liu and Ho.<sup>9</sup>

\* Fax: ++55 27 335 2823. E-mail: jair@cce.ufes.br.

† Universidade Federal do Espírito Santo.

‡ Centro Brasileiro de Pesquisas Físicas.

§ Universidade de São Paulo.

(1) Lee, J.-G.; Cutler, I. B. *Am. Ceram. Soc. Bull.* **1975**, *54*, 195.

(2) James, J.; Rao, M. S. *Am. Ceram. Soc. Bull.* **1986**, *65*, 1177.

(3) Krishnarao, R. V.; Godkhindi, M. M.; Mukunda, P. G. I.; Chakraborty, M. J. *Am. Ceram. Soc.* **1991**, *74*, 2869.

(4) Krishnarao, R. V.; Mahajan, Y. R. *Ceram. Int.* **1996**, *22*, 353.

(5) Real, C.; Alcalá, M. D.; Criado, J. M. *J. Am. Ceram. Soc.* **1996**, *79*, 2012.

(6) Weimer, A. R.; Cassidy, J. R.; Susnitzky, D. W.; Black, C. K.; Beaman, D. R. *J. Mater. Sci.* **1996**, *31*, 6005.

(7) Liou, T.-H.; Chang, F.-W.; Lo, J.-J. *Ind. Eng. Chem. Res.* **1997**, *36*, 568.

(8) Lanning, F. C. *J. Agric. Food Chem.* **1963**, *11*, 435.

(9) Liu, S.-L.; Ho, C.-H. *J. Chin. Chem. Soc. (Taiwan)* **1960**, *6*, 141.

(10) Yoshida, S.; Ohnishi, Y.; Kitagishi, K. *Soil Sci. Plant Nutr.* **1962**, *8*, 36.

(11) Sterling, C. *Am. J. Bot.* **1967**, *54*, 840.

(12) Sharma, N. K.; Williams, S.; Zangvil, A. *J. Am. Ceram. Soc.* **1984**, *67*, 715.

Nuclear magnetic resonance (NMR) spectroscopy has become a powerful tool in the research on solid organic and inorganic materials since the discovery of high-resolution techniques that made their spectra liquidlike.  $^{29}\text{Si}$  magic-angle spinning (MAS) NMR has been widely used in the investigation of structures in silica polymorphs,<sup>13</sup> SiC polytypes,<sup>14</sup> zeolites,<sup>15</sup> and many other inorganic materials.<sup>16,17</sup> A recent interest has developed in the use of  $^{29}\text{Si}$  MAS NMR to characterize the local structure of composite materials, such as polymer-derived ceramic fibers,<sup>18</sup> silica-carbon hybrids,<sup>19</sup> silicon oxycarbides,<sup>20</sup> silicon/carbon/nitrogen powders,<sup>21</sup> carbon-silicon alloy fibers,<sup>22</sup> and others. From such  $^{29}\text{Si}$  NMR spectra, one can identify the several chemical environments of silicon atoms in the material, because the nuclei belonging to chemically different species resonate at distinct frequencies (that is, they have their individual chemical shift). Moreover, it is possible to achieve quantitative information regarding the presence of silicon in different chemical structures, provided that the NMR spectrum is acquired with appropriate experimental parameters (noticeably, delay times).

In this work, we report the study of rice hulls, both raw and pyrolyzed, using high-resolution  $^{29}\text{Si}$  and  $^{13}\text{C}$  room temperature high-resolution solid-state NMR. Despite the wide applicability in ceramic materials, the use of NMR spectroscopy in the study of the occurrence and thermal transformations of silicon species in rice hulls has not been fully accomplished. One of the few recent reports using the NMR techniques related to rice hulls has been made by Hamdan et al.,<sup>23</sup> who used  $^{29}\text{Si}$  MAS NMR to investigate the synthesis of zeolites from rice hull ash. We also study here another biomass, the endocarp of babassu coconuts (*orbygnia martiana*), a typical Brazilian coconut that also contains silicon in its structure.<sup>24</sup> NMR spectroscopy is used in conjunction with X-ray diffraction (XRD) and scanning electron microscopy (SEM) in order to clarify the nature of silicon in these materials and follow the changes related both to the pyrolysis of the precursors and the formation of SiC from them, yielding important information about these processes.

## Experimental Section

**Preparation of Samples.** Samples of rice hulls and endocarp of babassu coconut (BC) were collected from southeast and northeast regions of Brazil, respectively. RH samples

were water-washed, dried at room temperature, and then cut in small pieces (around 5 mm long). BC samples were cut with a saw in small chips (about 1 cm long) separated from the endocarp of the coconut. Prior to the heat treatments, both sets of samples were dried at 105 °C in an oven. These samples were called natural RH and BC.

Heat treatments up to 1000 °C were performed inside a quartz tube under nitrogen atmosphere with a heating rate of 2 °C/min and a residence time of 1 h at each heat treatment temperature (HTT). About 5 g of raw material was used in these treatments, with mass yields of 30 and 28 wt % for RH and BC samples carbonized at 1000 °C, respectively. The treatments at higher HTTs (where the reaction of formation of SiC occurs) were performed in two steps: First, the natural RH and BC were treated under the conditions mentioned above at 700–900 °C for 2–4 h, to remove the volatile matter and produce a carbon-rich material. The resulting chars were then heat-treated within a high-purity alumina tube in a horizontal furnace up to HTTs between 1200 and 1450 °C. These heat treatments were performed under argon atmosphere with a heating rate of 5 °C/min and a residence time of 1–2 h at each final temperature.

**Sample Characterization.** XRD measurements were performed on powdered samples (<200 mesh), in a Siemens diffractometer using Cu K $\alpha$  radiation, with  $2\theta$  ranging from 10 to 90° in steps of 0.02°. SEM micrographs were achieved with a Cambridge LEICA S440I electronic microscope operating at 18 kV, with samples directly mounted on a copper basis.

**NMR Measurements.** NMR spectra were recorded at room temperature using a Varian INOVA 400 spectrometer, operating at 100.5 and 79.4 MHz for the  $^{13}\text{C}$  and  $^{29}\text{Si}$  nuclei, respectively. All experiments were realized with MAS, with a spinning frequency of about 5.0–6.0 kHz. High-power proton decoupling was used for the samples with low HTT (therefore, with high hydrogen content). Cross polarization (CP) or direct polarization (DP) was alternatively used, according to the specific character of each sample and the aim of the measurement. Chemical shifts, given in parts per million (ppm), for both  $^{13}\text{C}$  and  $^{29}\text{Si}$  nuclei were externally referred to tetramethylsilane (TMS). Adamantane (resonance line at 39.0 ppm from TMS in  $^{13}\text{C}$  NMR spectrum<sup>25</sup>) and kaolin (resonance line at -91.5 ppm from TMS in  $^{29}\text{Si}$  NMR spectrum<sup>26</sup>) were used for setting the reference frequency in  $^{13}\text{C}$  and  $^{29}\text{Si}$  NMR spectra, respectively.

For  $\{^1\text{H}-^{13}\text{C}\}$  CP/MAS NMR spectra, we used a proton  $\pi/2$  pulse width of 3.5  $\mu\text{s}$ , a contact time of 1 ms, and a recycle delay of 1.5 s. About 2000 transients were recorded, and a line broadening of 0–50 Hz was applied to the free induction decays (FIDs) before Fourier transform. Two  $^{13}\text{C}$  DP/MAS NMR spectra, with recycle delays of 5.0 and 50.0 s, respectively, were acquired for the sample RH 1450 °C, for which CP was not successful.  $\{^1\text{H}-^{29}\text{Si}\}$  CP/MAS NMR spectra were obtained with variable contact times (from 0.5 to 10 ms) and recycle delays (1.0 or 10.0 s). Proton  $\pi/2$  pulse widths and line broadening were similar to previous values and typically 5000 transients were acquired for each spectrum.  $^{29}\text{Si}$  DP/MAS NMR spectra were obtained with typical values of 3.8  $\mu\text{s}$  for the  $\pi/2$  pulse width, 2.0 or 10.0 s for the recycle delay, about 1200 for the number of transients, and 100 Hz for the line broadening.

For some particular samples, recycle delays were varied between 0.5 and 30.0 s and no remarkable effect of incomplete relaxation of the  $^{29}\text{Si}$  nuclei was observed. In well-crystallized materials, the use of much longer delays (on the order of minutes or hours) has been reported,<sup>14,21</sup> associated with the inefficient spin-lattice relaxation of  $^{13}\text{C}$  and  $^{29}\text{Si}$  nuclei. In our samples, otherwise, the possibility of using shorter recycle delays can be accounted for by the presence of paramagnetic centers in the disordered structure of pyrolyzed samples, which make more efficient the spin-lattice relaxation of the involved

(13) Smith, J. V.; Blackwell, C. S. *Nature* **1983**, *303*, 223.

(14) Hartman, J. S.; Richardson, M. F.; Sheriff, B. L.; Winsborrow, B. G. *J. Am. Chem. Soc.* **1987**, *109*, 6059.

(15) Fyfe, C. A.; Gobbi, G. C.; Hartman, J. S.; Lenkinski, R. E.; O'Brien, J. H. *J. Magn. Reson.* **1982**, *47*, 168.

(16) Turner, G. L.; Kirkpatrick, R. J.; Risbud, S. H.; Oldfield, E. *Am. Ceram. Soc. Bull.* **1987**, *66*, 656.

(17) Leone, E. A.; Curran, S.; Kotun, M.; Carrasquillo, G.; Van Weeren, R.; Danforth, S. C.; *J. Am. Ceram. Soc.* **1996**, *79*, 513.

(18) Lipowitz, J. *Ceram. Bull.* **1991**, *70*, 1888.

(19) Gilpin, R. K.; Gangoda, M. E.; Jaroniec, M. *Carbon* **1997**, *35*, 133.

(20) El Kortobi, Y.; d'Espinose de la Caillerie, J.-B.; Legrand, A.-P. *Chem. Mater.* **1997**, *9*, 632.

(21) El Kortobi, Y.; Sfihi, H.; Legrand, A.-P.; Musset, E.; Herlin, N.; Cauchetier, M. *Colloids Surf. A* **1996**, *115*, 319.

(22) Lu, S.; Rand, B.; Bartle, K. D.; Reid, A. W. *Carbon* **1997**, *35*, 1485.

(23) Hamdan, H.; Muhid, M. N. M.; Endud, S.; Listirini, E.; Ramli, Z. *J. Non-Cryst. Solids* **1997**, *211*, 126.

(24) Emmerich, F. G.; Luengo, C. A. *Biomass Bioenergy* **1996**, *10*, 41.

(25) Earl, W. L.; VanderHart, D. L. *J. Magn. Reson.* **1982**, *48*, 35.

(26) Wilson M. A. *NMR Techniques and Applications in Geochemistry and Soil Chemistry*; Pergamon Press: Oxford, 1987.

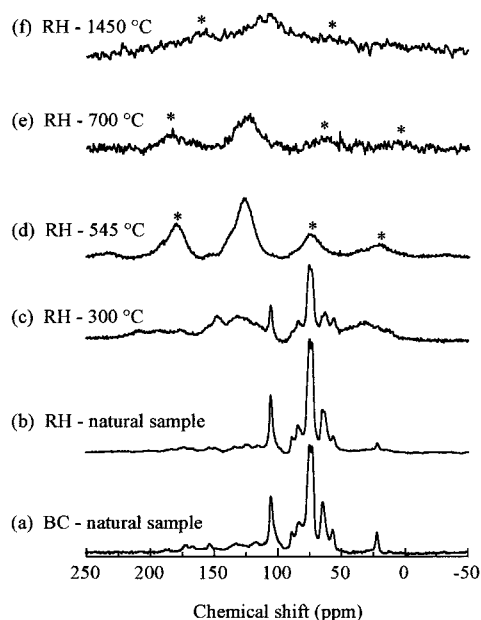


**Figure 1.**  $^{13}\text{C}$  NMR spectra of (a) natural BC sample, (b) natural RH sample, (c)–(f) RH samples carbonized at the indicated HTTs. Spectra were achieved with CP, except for the 1450 °C HTT RH sample (DP with recycle delay of 5.0 s). Stars denote spinning sidebands.

nuclei.<sup>20,27</sup> Therefore, although the lack of a precise knowledge of the spin–lattice relaxation times for the species studied here precludes the possibility of a reliable quantitative analysis, the spectra shown represent qualitatively well the silicon and carbon environments in the structure of the analyzed materials.

## Results and Discussion

**Natural RH and BC samples.** The  $^{13}\text{C}$  CP/MAS NMR spectra of the natural BC and RH samples are shown in parts a and b of Figure 1, respectively. One can depict in detail the lignocellulosic character of the organic part of these materials. Peaks from the main components of the structure of RH sample can be observed at 63.5, 65.0, 73.2, 75.5, 84.4, 89.3, and 105.8 ppm for cellulose; at 21.8 and 174.3 ppm associated with acetate groups of hemicellulose (besides those peaks in coincidence with cellulose); and at 56.8 and between 115 and 150 ppm (aromatic carbons) associated with lignin.<sup>28,29</sup> For BC sample, we can recognize the presence of nearly the same peaks, with little changes in position or intensity. In particular, we observe the higher intensity of the lignin peaks in the spectrum corresponding to the BC sample, evidencing the noticeably higher lignin content of this material.<sup>24</sup>

Natural RH and BC samples were found to have 3.47 and 0.38 wt % Si, respectively, from elemental analysis. The  $^{29}\text{Si}$  DP/MAS NMR spectra of these samples are shown in Figure 2 (bottom). Two resonance lines can easily be distinguished for both samples: a well-defined peak at  $-26$  ppm and a broad line centered around  $-112$  ppm with small shoulders in the region between  $-100$

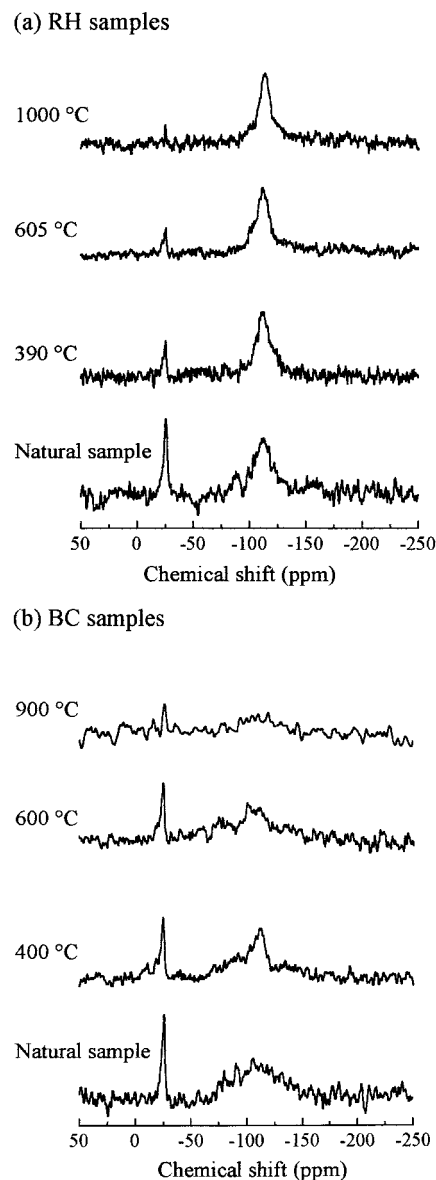


**Figure 2.**  $^{29}\text{Si}$  DP/MAS NMR spectra of natural and pyrolyzed (a) RH and (b) BC samples for various HTTs. Recycle delays were equal to 2.0 s for natural RH and BC samples and to 10.0 s for pyrolyzed samples.

and  $-90$  ppm. In the spectrum of the BC sample, the latter line is broader than that in the RH case. Both spectra were acquired with a recycle delay of 2.0 s. Some tests were performed using longer recycle delays (up to 30.0 s), and it was verified a small increase in the relative intensity of the line around  $-112$  ppm, indicating a slower spin–lattice relaxation for this line.

Chemical shifts ranging from  $-90$  to  $-115$  ppm are typical of silicate groups, where silicon atoms are surrounded in a tetrahedral arrangement by four oxygen atoms at the first coordination sphere, constituting the so-called Q units. The exact position of the resonance line for a given species is determined by the presence of other atoms at the following coordination spheres and by crystalline organization effects.<sup>13,20</sup> The chemical shift around  $-110$  ppm is attributed to the group  $\text{Si}^*$  ( $\text{OSi})_4$  ( $\text{Q}^4$  unit), whereas resonance lines corresponding to  $\text{Q}^3$ ,  $\text{Q}^2$ ,  $\text{Q}^1$ , and  $\text{Q}^0$  units are progressively shifted to the lower shielding direction by roughly 10 ppm each (the superscripts indicate the number of siloxane

(27) Pan, H.; Pruski, M.; Gernstein, B. C.; F. Li, Lannin, J. S. *Phys. Rev. B* **1991**, *44*, 6741.

(28) Kolodziejewski, W.; Frye, J. S.; Maciel, G. E. *Anal. Chem.* **1982**, *54*, 1419.

(29) Solum, M. S.; Pugmire, R. J.; Jagtoyen, M.; Derbyshire, F. *Carbon* **1995**, *33*, 1247.

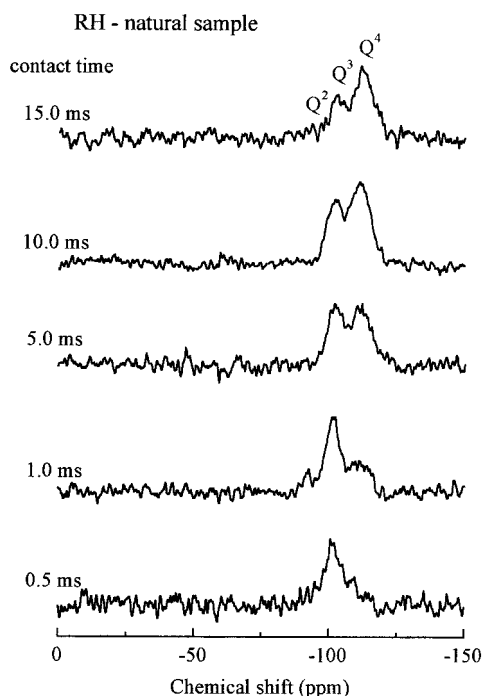


**Figure 3.**  $^{29}\text{Si}$  CP/MAS NMR spectra of natural RH sample achieved with variable contact times, as indicated.

bonds).<sup>26</sup> On the basis of these assignments, the broad line appearing in the natural samples spectra shown in Figure 2 near  $-112$  ppm can be associated with  $\text{Si}^*(\text{OSi})_4$  groups, with the shoulders in the lower shielding side being possibly due to  $\text{Q}^3$  and  $\text{Q}^2$  units (as it will be discussed below, in connection with CP measurements). The shape of the resonance in this region, broad and poorly defined, particularly in the spectrum corresponding to the BC sample, is in accordance with what is expected for an amorphous form of silica (see XRD results below).<sup>23</sup>

The narrow line at  $-26$  ppm, which is present in the spectra of both RH and BC samples, is of a completely different nature. Its chemical shift lies in the region where one normally finds the resonance due to silicon atoms bound to carbon atoms. Thus, this line is associated with silicon species taking part of the organic structure of the material; its existence constitutes, at least to authors' knowledge, the first *direct* evidence of the bonding of silicon to organic groups in biomass materials, confirming the ideas of Liu and Ho<sup>9</sup> and Sharma et al.<sup>12</sup> There are several reports about silicon in  $\text{Si}^*(\text{C}_2\text{O}_2)$  groups giving rise to resonance lines between  $-18$  and  $-35$  ppm;<sup>18,20</sup> in addition, Horn and Marsman<sup>30</sup> described a series of organosilicon compounds of the type  $\text{Si}(\text{CH}_3)_2\text{O}[\text{Si}^*(\text{CH}_3)_2\text{O}]_n\text{Si}(\text{CH}_3)_2\text{OH}$  with chemical shifts close to  $-24$  ppm, for various degrees of polymerization (different values of  $n$ ). Therefore, the occurrence of the narrow line shown in Figure 2 suggests that a chemical environment similar to this can be found for silicon species in biomass materials.

To obtain additional information about this subject, we performed some CP experiments with variable contact times. The results are shown in Figure 3 for the RH sample; similar findings were obtained for the BC sample. We can see that the broad resonance associated

with the Q units is in fact composed of at least two separate lines, with distinct behavior in the variable contact time experiment. There is a line near  $-102$  ppm, in the range of the  $\text{Q}^3$  units, that is easily cross-polarized, even for the short contact time of  $0.5$  ms. With the increase in the contact time, the  $\text{Q}^4$  line previously found in the DP spectrum at  $-112$  ppm arises, indicating a site with slower polarization rate. For the highest values of contact times used, this line exhibits an intensity higher than that of the line at  $-102$  ppm, resembling the shape of the DP spectrum and indicating that the major part of the silicon species belong in fact to the  $\text{Q}^4$  environment. In addition, we can observe small signals little above the noise level around  $-90$  ppm, probably associated with  $\text{Q}^2$  units.

In the CP dynamics, we can say that the optimum value of the contact time for each resonance line lies, in the ideal case, well above  $T_{\text{SiH}}$  (the cross-polarization time) and well below  $T_{1\rho\text{H}}$  (the proton rotating-frame spin-lattice relaxation time). The understanding about these parameters, obtained through the analysis of the results of CP experiments with variable contact times, allows the achievement of information about the magnitude of  $^{29}\text{Si}-^1\text{H}$  dipolar interaction, the mobility of the involved molecules, and the possible presence of paramagnetic impurities near them.<sup>26</sup> Following this reasoning, we can interpret the behavior exhibited in the sequence of spectra shown in Figure 3, which is similar to various results referring to gels and other forms of silica.<sup>23,31,32</sup> The  $\text{Q}^4$  line at  $-112$  ppm corresponds to silicon atoms in  $\text{Si}^*(\text{OSi})_4$  groups, removed from the nearest hydrogen atom by at least four bond distances; this explains the slow polarization rate observed in the CP dynamics for this line. The outset of the line at  $-102$  ppm with high intensity in the CP spectra is typical of hydroxyl-containing  $\text{Q}^3$  units;<sup>32</sup> this line can thus be ascribed to  $(\text{HO})\text{Si}^*(\text{OSi})_3$  moieties, where the central silicon atom is directly bound to one hydroxyl group and therefore is susceptible to a more efficient mechanism of magnetization transference. The presence of hydroxyl groups near or attached to silicon tetrahedra, demonstrated by the CP spectra, is in accordance with the commonly accepted conclusion that silica in rice hulls occurs in a hydrated form.<sup>8,12</sup> In addition, Maciel and Sindorf,<sup>31</sup> in a study about surface groups in silica gel, reported  $T_{\text{SiH}}$  values of  $2.9$  and  $12.7$  ms for  $\text{Si}^*(\text{OSi})_4$  and  $(\text{HO})\text{Si}^*(\text{OSi})_3$  moieties, respectively, and  $T_{1\rho\text{H}}$  values around  $21$  ms for both. These findings agree qualitatively well with the results presented in Figure 3 and with the interpretation given here for them.

A fact of remarkable importance that emerges from the analysis of the spectra presented in Figures 2 and 3 is the lack of any signal near  $-26$  ppm in the CP spectra of Figure 3, where there was a narrow well-defined peak in the DP spectra presented in Figure 2. This means that the  $^{29}\text{Si}$  nuclei responsible for that resonance line, which were associated with silicon atoms bound to organic groups, belong to an environment where the CP process is completely inefficient under the experimental conditions here used. We made some tests changing the contact times and recycle delays in the CP

(31) Maciel, G.; Sindorf, D. W. *J. Am. Chem. Soc.* **1980**, *102*, 7607.

(32) Abidi, N.; Deroide, B.; Zanchetta, J. V.; De Menorval, L. C.; d'Espinose, J. B. *J. Non-Cryst. Solids* **1998**, *231*, 49.

(30) Horn, H.; Marsmann, H. C. *Makromol. Chem.* **1972**, *162*, 1972.

experiment in order to verify the possible occurrence of that signal, but all trials revealed no line near  $-26$  ppm.

There are some possible explanations for the nonexistence of this CP signal. One possibility is that one is dealing with a site near a paramagnetic center, which shortens  $T_{1\rho\text{H}}$  so much that it is impossible to perform the transference of magnetization from protons to  $^{29}\text{Si}$  nuclei. Although this fact is very common in coals<sup>33</sup> and pyrolyzed organic materials,<sup>34</sup> due to the existence of paramagnetic centers such as mineral magnetic impurities or free radicals, its occurrence in a natural biomass material like RH or BC is quite unlikely. Another possibility is that the involved  $^{29}\text{Si}$  nuclei are far apart from the nearest protons, so that  $T_{\text{SiH}}$  assumes excessively high values that make impossible the realization of CP. On the basis of the assignment previously made, this possibility also appears to be improbable. That is because the natural biomass materials are abundant in hydrogen and, since the  $^{29}\text{Si}$  nuclei corresponding to the  $-26$  ppm resonance must be associated with groups attached to the organic part of the material, the silicon atoms involved are almost certainly bound to protonated carbons, like the methyl groups mentioned above, and therefore are not sufficiently removed from protons.

We think the more feasible reason for the inefficiency of CP is that the protons near the  $^{29}\text{Si}$  nuclei in the chemical group under discussion belong to a nonrigid environment. Therefore, the high mobility of this group (the methyl group, for example, in our previous assignment) would average out the dipolar interaction between  $^{29}\text{Si}$  nuclei and protons, leading to an inefficient polarization transfer. The occurrence of problems with CP for  $^{13}\text{C}$  nuclei belonging to groups that undergo rapid molecular motion has been reported in organic materials.<sup>26,33</sup> If it happened for the  $^1\text{H}$ – $^{29}\text{Si}$  interaction in the case reported here, this fact might be the cause of the inefficiency of CP and could therefore explain the lack of signals from organosilicon groups in the  $^{29}\text{Si}$  CP/MAS NMR spectra of Figure 3.

**Pyrolyzed Samples.** The  $^{13}\text{C}$  CP/MAS NMR spectra of the pyrolyzed RH samples are shown in Figure 1c–f for various HTT; similar results were obtained for the BC samples. These spectra reveal the progress of the carbonization process, showing the evolution of the lignocellulosic original composition toward a highly aromatic structure.<sup>29,34</sup> Initially, we can recognize the degradation of carbohydrates, with the progressive breakdown of the peaks associated with cellulose and hemicellulose. For HTT above  $\sim 500$  °C, only one well-defined aromatic line is observed, with a chemical shift about 125 ppm and a good S/N ratio, pointing to an efficient realization of CP for carbon atoms locally organized in graphitic-like planes. The occurrence of several spinning sidebands, marked by stars in the spectra, indicates a large chemical shift anisotropy, typical of aromatic carbons. The CP process was efficient up to HTT of about 700 °C. For higher HTTs, the CP signal became very poor due to the low hydrogen content of these samples, so we used the DP method. The DP

spectrum of the 1450 °C HTT sample exhibits a very broad aromatic line shifted to the higher shielding direction. This constitutes an indication that a larger portion of the carbon atoms in the material, with enhanced chemical shift anisotropy, are being detected with the DP technique, in comparison with those in the CP spectra.<sup>34</sup>

In Figure 2a, we show the evolution of the  $^{29}\text{Si}$  DP/MAS NMR spectra for the RH-pyrolyzed samples, achieved with a recycle delay of 10.0 s. We can observe clearly the progressive decrease in intensity of the line at  $-26$  ppm, up to 1000 °C. Simultaneously, the resonance around  $-112$  ppm becomes more pronounced, indicating that the chemical and physical changes accompanying the pyrolysis of the material lead to the conversion of the organically bound silicon species into the oxygenated Q units previously described. Furthermore, we can note the improvement in the S/N ratio for this resonance with the increasing in HTT. This can be due to the shortening of the spin–lattice relaxation time for the  $^{29}\text{Si}$  nuclei in this environment, caused by the gradually higher number of lattice defects in the structure of the material with the progress of pyrolysis.<sup>20,27</sup> The short recycle delays here used do not appear to be sufficient for the full spin–lattice relaxation of the  $^{29}\text{Si}$  nuclei in the Q units in the natural samples, as cited previously. However, it seems that the existence of paramagnetic defects in the disordered structure of the pyrolyzed samples leads to a more efficient spin–lattice relaxation for the  $^{29}\text{Si}$  nuclei, explaining the behavior mentioned above. These defects are produced during the course of pyrolysis as consequences of the breakdown reactions in the structure of the organic precursor, leading to the formation of stable free radicals. This subject has been investigated largely through electron paramagnetic resonance (EPR) in carbonized lignocellulosic precursors and other heat-treated materials, and it constitutes the main mechanism for spin–lattice relaxation in NMR measurements.<sup>21,27,35</sup>

In Figure 2b, the  $^{29}\text{Si}$  DP/MAS NMR spectra of the BC-pyrolyzed samples are presented. The observed behavior is in many aspects similar to the RH samples, although the S/N ratios are worse in the BC case due to the lower Si content of this material. (Elemental analysis yielded 13.41 and 1.35 wt % of Si for RH and BC samples pyrolyzed at 900 °C, respectively.) One important difference that we can note in the NMR spectra of the BC compared to those of the RH samples is the relatively higher intensity of the line at  $-26$  ppm, which is kept in some cases even more intense than the broad line near  $-112$  ppm. With the increase in HTT, the diminishment in intensity of the line associated with organically bound silicon species is also observed, in accordance with the behavior exhibited by the RH-pyrolyzed samples.

The  $^{29}\text{Si}$  CP/MAS NMR spectra of both BC- and RH-pyrolyzed samples (not shown) are similar to the CP spectra of the natural samples previously presented in Figure 3. The line at  $-26$  ppm is not again observed, whereas the easily detectable resonance associated with Q units is constituted of two lines with distinct CP dynamics. The CP process was efficient up to HTT =

(33) Snape, C. E.; Axelson, D. E.; Botto, R. E.; Delpuech, J. J.; Tekely, P.; Gernstein, B. C.; Pruski, M.; Maciel, G. E.; Wilson, M. A. *Fuel* **1989**, *68*, 547

(34) Freitas, J. C. C.; Bonagamba, T. J.; Emmerich, F. G. *Energy Fuels* **1999**, *13*, 53.

(35) Emmerich, F. G.; Rettori, C.; Luengo, C. A. *Carbon* **1991**, *29*, 305.

605 °C; the low hydrogen content of the samples pyrolyzed at higher temperatures made impossible the achievement of CP spectra for them.

The existence of organically bound silicon species in the structure of well-carbonized samples, identified by the peak at  $-26$  ppm in the spectra of Figure 2, constitutes additional evidence about the nature of silicon in biomass materials. It has been suggested in previous reports<sup>9,12</sup> that silicon species in natural RH are in part combined with carbohydrates (cellulose and hemicellulose). However, the analysis of the  $^{13}\text{C}$  NMR spectra previously presented shows clearly that carbohydrates are completely decomposed at HTT around 300–400 °C, in accordance with results of similar studies about pyrolysis in other organic materials.<sup>29,34</sup> This can be seen in Figure 1 in the spectrum corresponding to the 545 °C HTT sample, where no line from carbohydrates is present. Thus, it appears from the persistence of the line at  $-26$  ppm in our spectra of Figure 2 for HTT  $\sim 600$  °C and, with smaller intensity, for HTT up to 1000 °C that the organically bound silicon species are not, at least not in the whole part, connected to carbohydrates. It seems to be more appropriate to suppose that these species occur in association with the more thermally stable lignin groups, possibly linked to side-chain groups. With the sequence of carbonization, the organically bound silicon moieties would take part in the cross-links<sup>36</sup> imbedded in the aromatic carbon network. A further support for this inference is the higher relative intensity of the line near  $-26$  ppm in the  $^{13}\text{C}$  NMR spectra of the BC samples (Figure 2b) in comparison to the RH samples (Figure 2a). In fact, BC is known to possess a remarkably high lignin content,<sup>24</sup> which, according to the reasoning outlined above, would lead to a relatively intense peak corresponding to the organically bound silicon species. From these results, we can conclude that silicon in BC and RH samples occurs in great part in the form of organically bound moieties, probably in association with side-chain lignin groups, which are preserved (mostly for BC samples) at HTT as high as 1000 °C.

The analysis of the  $^{13}\text{C}$  and  $^{29}\text{Si}$  NMR spectra of the pyrolyzed samples allows us to identify the structure of the carbonized samples, with HTT around 1000 °C, as consisting of aromatic planes of carbon atoms in a more or less organized arrangement. In this HTT range, as we will see later through the analysis of XRD spectra, there is no long-range spatial ordering in the structure of the material. Dispersed throughout the organic matrix, there are aggregates of silicon species, some of them (the major part, in the RH case) constituting the amorphous silica tetrahedra and others still bound to the organic part of the material.

**Formation of SiC.** From the intimate mixture of carbon and silica reported above, one was able to conduct the heat treatments for the production of SiC at temperatures up to 1450 °C. This process can be analyzed from the XRD spectra of the RH samples shown in Figure 4. In the sample with HTT = 700 °C, used as precursor for the subsequent reactions at higher temperatures, we can verify the amorphous character of the starting material. Only the broad reflections from

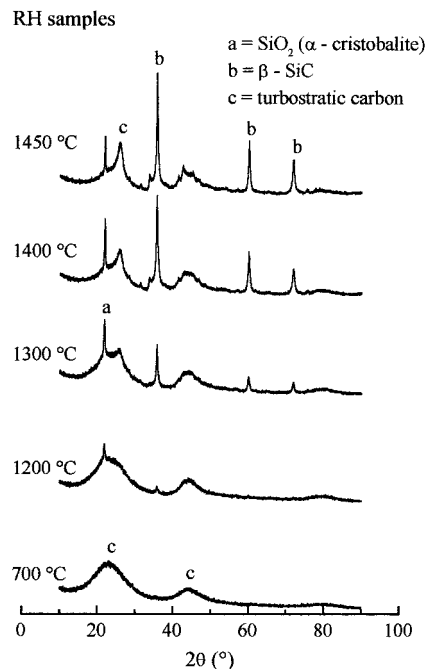
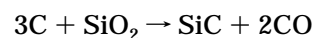


**Figure 4.** XRD spectra of RH samples for the indicated HTTs. The identified phases are displayed.

the carbon turbostratic structure<sup>37</sup> can be observed, located near  $2\theta = 23$  and  $43^\circ$ . The reflections from amorphous silica occur around  $22^\circ$ ,<sup>8</sup> being therefore superimposed to the turbostratic broad lines.

From 1200 °C upward, we can observe the crystallization of silica in the  $\alpha$ -cristobalite phase, identified by the narrow peak at  $21.9^\circ$ ,<sup>3,12</sup> as well as the formation of SiC in the cubic phase ( $\beta$ -SiC), characterized by the peaks at  $35.7$ ,  $60.1$ , and  $71.8^\circ$ .<sup>3,38</sup> The intensities of the SiC peaks increase progressively, particularly above 1300 °C, when the peak of cristobalite starts to decrease, reflecting the progress of SiC formation. In the 1450 °C HTT sample, we observe the coexistence of well-crystallized SiC with remnant crystalline silica and amorphous carbon phases. The gradual narrowing and the high-angle shifting of the line associated with the turbostratic structure of the carbon-rich phase (appearing at  $25.8^\circ$  for the 1450 °C HTT sample) characterize the progressive organization of the carbon graphite-like network. This process occurs however in a limited way, because the hard structure originated from the lignocellulosic precursor makes the material nongraphitizable.<sup>37</sup> BC samples presented qualitatively the same behavior under XRD measurements, but with the formation of SiC occurring in lower amount and at temperatures higher than those for RH samples.

The overall reaction governing the formation of SiC from the carbothermal reduction of silica can be written as



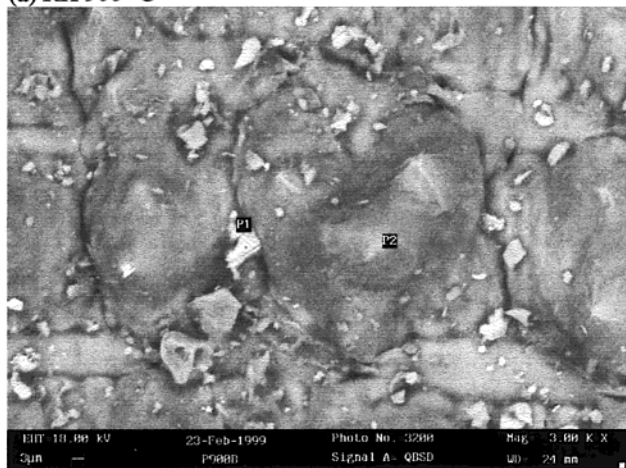
Four competitive processes are described to take place related to this reaction: crystallization of amorphous silica to cristobalite, partial graphitization of amorphous

(36) Walker, P. L., Jr. *Carbon* **1986**, *24*, 379.

(37) Van Krevelen, D. W. *Coal: Typology, Chemistry, Physics, Constitution*; Elsevier: Amsterdam, 1993.

(38) Tougne, P.; Hommel, H.; Legrand, A. P.; Herlin, N.; Luce, M.; Cauchetier, M. *Diamond Relat. Mater.* **1993**, *2*, 486.

(a) RH 900 °C



(b) RH 1450 °C

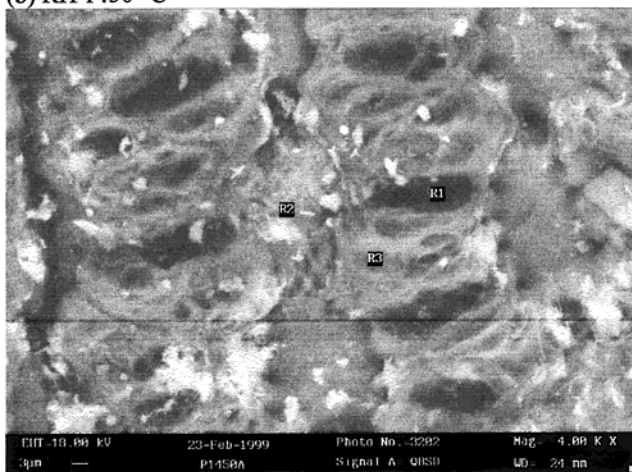


**Figure 5.** SEM images of RH samples heat-treated at (a) 900 and (b) 1450 °C.

carbon, formation of SiC polycrystals, and formation of SiC whiskers.<sup>3,4</sup> The crystallization of both silica and carbon are barriers to the SiC formation because the amorphous species are more reactive.<sup>1,7,39</sup> Although the graphitization of carbon is limited here, as described above, the crystallization of cristobalite in fact takes place as we have detected from XRD data. Its occurrence in the 1450 °C HTT sample indicates that the reaction of production of SiC was not complete in our samples. The use of higher heating rates starting directly from raw precursors has been reported as a means of avoiding the silica crystallization and therefore could lead to an increase in the amount of SiC produced.<sup>39</sup>

The morphology of RH samples heat-treated at 900 and 1450 °C can be analyzed from the SEM images exhibited in Figure 5. The appearance of the samples is similar to those in previous reports.<sup>4,12</sup> In the image of the 900 °C HTT sample (Figure 5a), we can see a smooth surface with several small grains. Energy-dispersive spectrometry (EDS) analysis performed at the points P1 and P2 indicated in the figure shows the presence of potassium oxide (a common impurity in not-acid-leached rice hulls<sup>7</sup>) at the small white particle P1 and large concentrations of silicon and carbon around

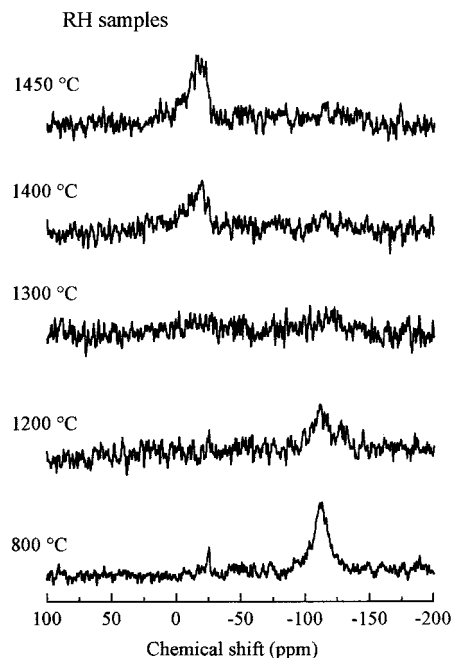


**Figure 6.** <sup>29</sup>Si DP/MAS NMR spectra of pyrolyzed RH samples for various HTTs, acquired with 10.0 s recycle delay.

the gray protuberances around P2. In the image of the 1450 °C HTT sample displayed in Figure 5b, we observe the changes associated with the formation of SiC and the crystallization of silica: large white regions can be distinguished, around the point R2, for example, consisting of both cristobalite and  $\beta$ -SiC. Around R1 and R3 positions, carbon was found to have the larger concentration, although some silicon has been observed in both points. SiC whiskers can also be observed in the figure, noticeably near the lower right corner.

The <sup>29</sup>Si DP/MAS NMR spectra of the RH samples heat-treated above 1000 °C showed poor S/N ratios; these spectra are shown in Figure 6, together with the spectrum of a lower HTT sample (800 °C) for comparison, in a sequence similar to that presented in Figure 4 for XRD data. The NMR spectrum of the 800 °C HTT sample, which has an amorphous structure, exhibits two well-distinguished resonance lines, as discussed above, with a relatively good S/N ratio. From 1200 °C upward, the quality of the spectra becomes inferior. The resonance associated with Q units is present in the 1200 °C HTT sample spectrum (together with some signals from organically bound silicon species), but it can hardly be distinguished in the subsequent NMR spectra, despite the large amount of cristobalite identified in the XRD spectra. The main reason for the poor quality of these spectra is the organization of the silicon-containing species in crystalline regions previously identified as cristobalite and  $\beta$ -SiC. Consequently, the spin-lattice relaxation time of the <sup>29</sup>Si nuclei belonging to these regions becomes longer, as expected for crystalline materials,<sup>14,21</sup> and the short delay times here used become ineffective for the full spin-lattice relaxation of these nuclei. This explains the presence of some intensity around -112 ppm for the 1200 °C HTT sample, where the crystallization of cristobalite is restricted as seen in Figure 4, whereas for the higher HTT samples, with larger extent of crystalline organization, this intensity is almost imperceptible.

(39) Krishnarao, R. V.; Subrahmanyam, J.; Mohanarao, R.; Jagdishkumar, T. *J. Mater. Synth. Process.* **1996**, *4*, 285.

The line associated with SiC, located around  $-18$  ppm, is easily observed for HTT = 1400 and 1450 °C (and for 1300 °C in a smaller extent), in accordance with the XRD results. No splitting of this line due to crystallographically distinct silicon sites was observed, which is coherent with the previous identification of the SiC phase as being cubic ( $\beta$ -SiC).<sup>14</sup> The  $^{29}\text{Si}$  nuclei in this environment appear to have a faster relaxation dynamics when compared to those of Q units;<sup>21</sup> we acquired NMR spectra for the 1400 °C HTT sample with recycle delays from 2 to 30 s, and the line near  $-18$  ppm was always observed with a reasonable S/N ratio after about 1000 scans. In contrast, no evident signal from SiC was perceptible in the  $^{13}\text{C}$  NMR spectra of the 1450 °C HTT sample (see Figure 1) for recycle delays between 5.0 and 50.0 s, confirming the reports of Hartman et al.<sup>14</sup> of prohibitively long spin-lattice relaxation times for  $^{13}\text{C}$  nuclei in cubic SiC environments.

### Conclusions

$^{29}\text{Si}$  high-resolution solid-state NMR was successfully used to investigate the occurrence of silicon in two kinds of biomass (rice hulls and endocarp of babassu coconut). The combination of CP and DP methods in the natural samples led to the identification of two quite different chemical environments for silicon. The first one was associated with silicon atoms bound in a tetrahedral arrangement to other silicon atoms through oxygen bridges; the presence of hydroxyl groups near or bound to these silicon atoms confirmed the hydrated nature of these silica species. The second chemical environment revealed by NMR measurements was ascribed to organically bound silicon species, for which the CP process was completely inefficient under the experimental conditions here used. This suggested the possibility of a sufficiently high mobility for the protonated part of the group, so that the average dipolar interaction between protons and  $^{29}\text{Si}$  nuclei would be reduced and the transference of polarization would be inefficient. The occurrence of the same resonance line (near  $-26$  ppm) in both materials studied here might be an indication of a general type of chemical bonding between silicon and organic groups in natural biomass.

The study of pyrolyzed samples, both through  $^{13}\text{C}$  and  $^{29}\text{Si}$  NMR, allowed the understanding of the changes occurring in the materials upon heat treatments. Short recycle delays could be used due to the disordered character of the samples, which hastened the spin-lattice relaxation of  $^{29}\text{Si}$  nuclei. With increasing HTT, the organic part became progressively more aromatic, with a complete breakdown of carbohydrates at temperatures around 300–400 °C. For the silicon species, the heat treatments led to an increase in the relative intensity associated with oxygenated silicon and to a progressive diminishment of the line corresponding to organically bound silicon moieties. However, the latter line could be observed at HTT as high as 1000 °C (noticeably for BC samples, with high lignin content), although with reduced intensity. This fact suggested that these silicon species were not connected to carbohydrates, at least not in the whole part; they were probably associated with side-chain lignin groups in the natural samples, taking part in the cross-links imbedded in the aromatic network during the sequence of carbonization.

The formation of SiC was accomplished through heat treatments performed above 1200 °C. XRD and SEM showed the conversion of the initially amorphous material in a mixture of crystalline  $\alpha$ -cristobalite and  $\beta$ -SiC with turbostratic carbon. As usual, SiC whiskers were identified in the 1450 °C HTT sample. The NMR spectra of the samples with HTT from 1200 °C upward showed the progressive appearance of the SiC line, in accordance with XRD results, although the S/N ratio has become too poor due to the increase in spin-lattice relaxation times for  $^{29}\text{Si}$  nuclei in the well-crystallized samples.

**Acknowledgment.** This work was partially supported by Brazilian agencies CNPq, CAPES, FINEP, and FAPESP. The authors are grateful to the CST Corporation for SEM micrographs, to Dr. M. F. Sousa for providing RH samples, and to MSc M. T. D. Orlando for his collaboration in the performance of XRD measurements. The text was improved by the comments and suggestions of the anonymous reviewers.

CM990472G